esteem3

Enabling Science through European Electron Microscopy

Second report on TEM methods applied to materials for health

Deliverable D9.2 – version 2.1

Estimated delivery date: 31.12.2021

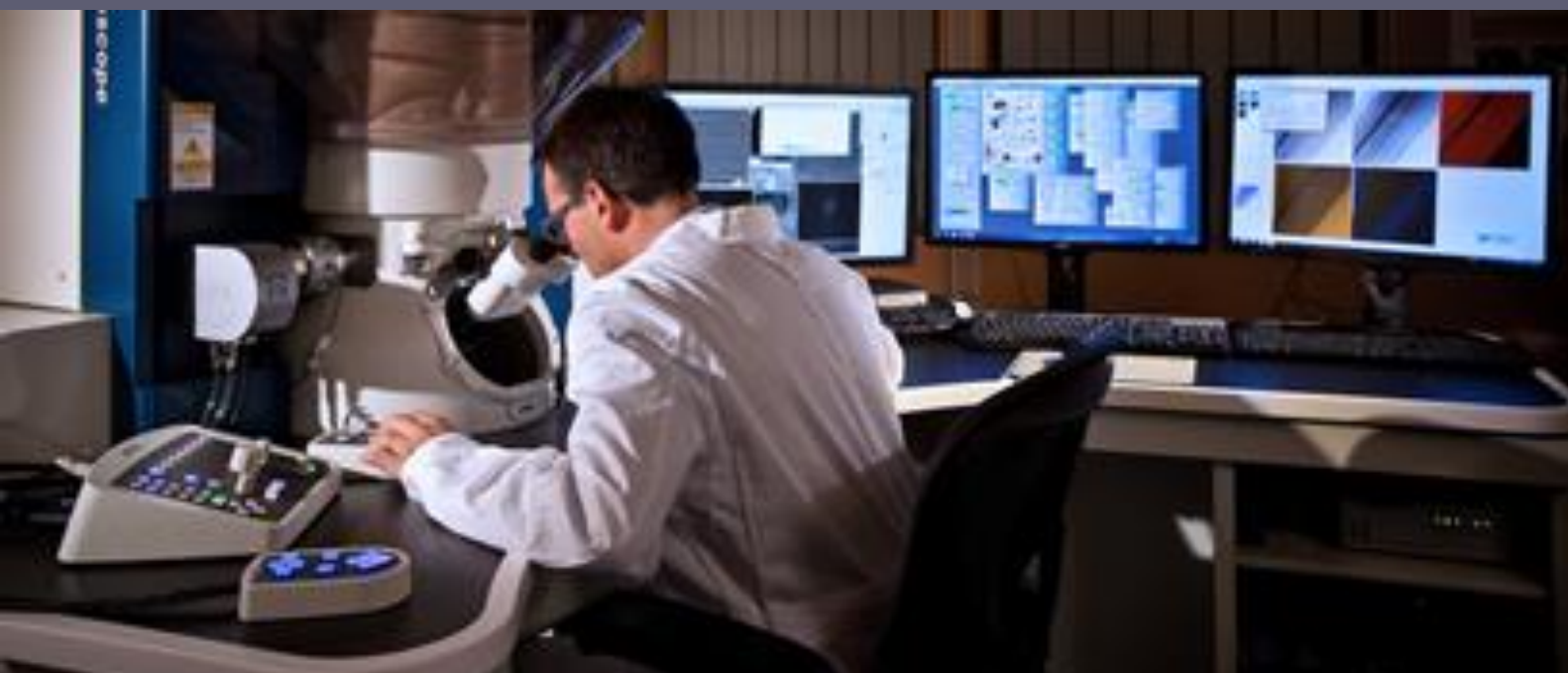Actual delivery date: 01.12.2021

Lead beneficiary: STU

Person responsible: Vesna Srot

Deliverable type: ☒ R ☐ DEM ☐ DEC ☐ OTHER ☐ ETHICS ☐ ORDP

Dissemination level: ☒ PU ☐ CO ☐ EU-RES ☐ EU-CON ☐ EU-SEC

Grant Agreement No:	823802
Funding Instrument:	Research and Innovation Actions (RIA)
Funded under:	H2020-INFRAIA-2018-1: Integrating Activities for Advanced Communities
Starting date:	01.01.2019
Duration:	54 months

Table of contents

Revision history log

Version number	Date of release	Author	Summary of changes
V0.1		Vesna Srot	First draft
V1.1	30/11/2021	Aude Garsès	General review
V1.2	30/11/2021	Vesna Srot	Minor changes
V2.1	01/12/2021	Peter A. van Aken	Final approval

Revision history log

Exxecutive Summary

This report summarises projects performed in STU, UOXF and ANT within the WP9 – Materials for Health.

Sample preparation of organic/inorganic materials (STU)

TEM sample preparation of organic/inorganic composite materials is a highly delicate and demanding task. Organic and inorganic components have different mechanical, physical and chemical properties and therefore diverse polishing and milling rates. It is well known that the quality of TEM samples is often a limiting factor for successful electron microscopy investigations. We have optimized the preparation of electron-transparent foils from dentine areas in rodent incisors and molar teeth by ultramicrotomy (Figure 1) and FIB technique (Figure 2).
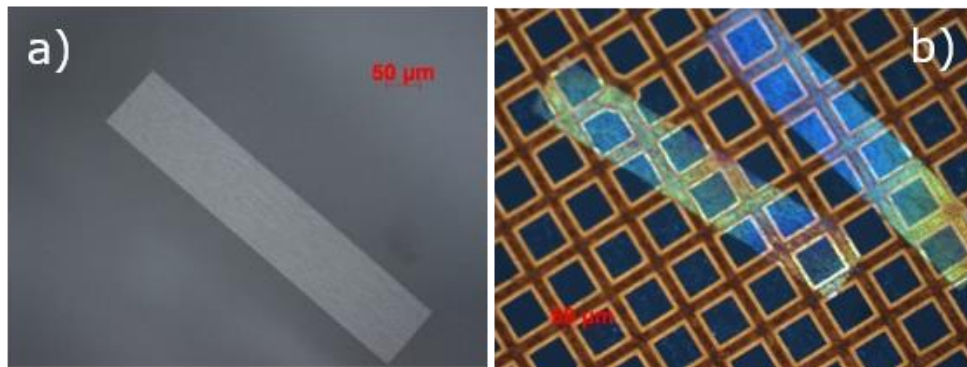

Figure 1: Ultramicrotomy sample preparation of rodent dentine. (a) Block face and (b) electron-transparent slices deposited on a Cu grid.
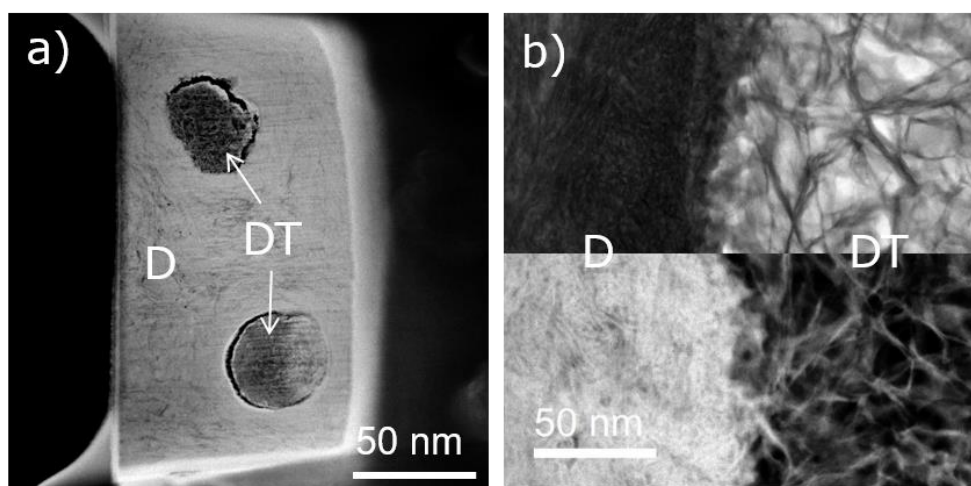

Figure 2: FIB sample preparation of rodent dentine. (a) HAADF-STEM, (b) BF-STEM (top) and HAADF-STEM (bottom) images with marked positions of dentinal tubules (DT) and dentine (D).

The FIB lamellae from rodent dentine (Figure 2) was prepared in a plan-view orientation from the block face that was initially prepared by ultramicrotomy. For biological samples, surfaces prepared with an ultramicrotome offer better quality compared to classical polished surfaces. For this purpose, we have developed a new protocol that will be published in a research paper and on the ESTEEM3 webpage once the characterization of the samples will be finalized.

Studies of environmental pathologies on enamel are important for better understanding of the origins of diseases. Since such affected areas are site specific, we have developed a FIB protocol for preparation of sensitive biological samples from site-specific areas. We are currently working on the preparation of FIB samples from different areas of diseased human and rodent teeth. Afterwards, the samples will be characterized by TEM and the findings and protocol will be published in a research paper and on the ESTEEM3 webpage.

In Figure 3, a diseased human tooth is presented. A FIB lamellae was prepared from an area, where stripes are clearly visible on the tooth surface (yellow square). BF-STEM images (Figure 4) show a cross-sectional view of such a diseased area.

Figure 3: FIB sample preparation of dental pathologies. Presented is a diseased human tooth. FIB sample shown in Figure 4 was prepared from an area marked with the yellow square (right image).
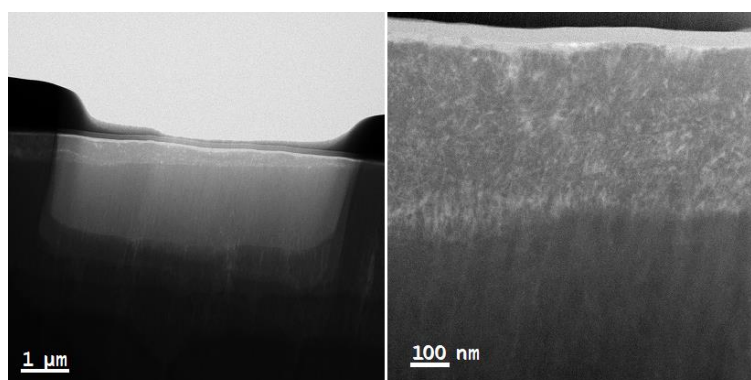

Figure 4: FIB sample preparation of dental pathologies. BF-STEM images from the site-specific area (marked with a yellow square in Figure 3) of a diseased human tooth.

We have been constantly working on improvement of sample preparation of such composite organic/inorganic materials where different techniques and their combinations are successfully used.

Clustering of Pt in platin-dosed cells (UOXF)

Oxaliplatin is a first-line chemotherapeutic used to treat a number of cancers. Its structure contains a single atom of platinum, which preferentially binds to DNA and causes cell death. However, there are numerous side effects associated with oxaliplatin treatment. One of the most clinically challenging of these is oxaliplatin induced peripheral neuropathy (OIPN). This causes pain and numbness in the extremities, which at present cannot be alleviated or prevented. OIPN is a primary reason for discontinuation of an otherwise effective chemotherapeutic regimen, which can impact on patient quality of life and survival. Here, we show how quantitative ADF STEM methods may be adapted for subcellular elemental characterization and used to localize single atoms of platinum (Pt) within neuronal cell bodies, following *in vivo* administration of the Pt-based chemotherapeutic oxaliplatin.

Mass spectrometry studies on homogenized whole tissues have shown that the dorsal root ganglion (DRG) is site of oxaliplatin accumulation. Whole rat DRG were recovered following prolonged *in vivo* oxaliplatin administration. Following light fixation overnight using a 0.5% formaldehyde solution, the DRG were placed in a 2.3M sucrose solution and before being plunge frozen and stored in liquid nitrogen. Ultrathin samples of frozen DRG were then sectioned by cryo-ultramicrotomy. Sections were then transferred to pioloform-coated copper TEM grids using a 50:50 1% methylcellulose-2.3M sucrose solution, which acted to embed the sample in a thin polymer layer. Sections and grids were subsequently thawed on the bench to produce high-quality samples with identifiable ultrastructure, which were stable at room temperature.

In ESTEEM3 Report D9.1, we showed that single Pt atoms could be identified in the observed in the DRG neuronal cell body cytosol (Figure 5).
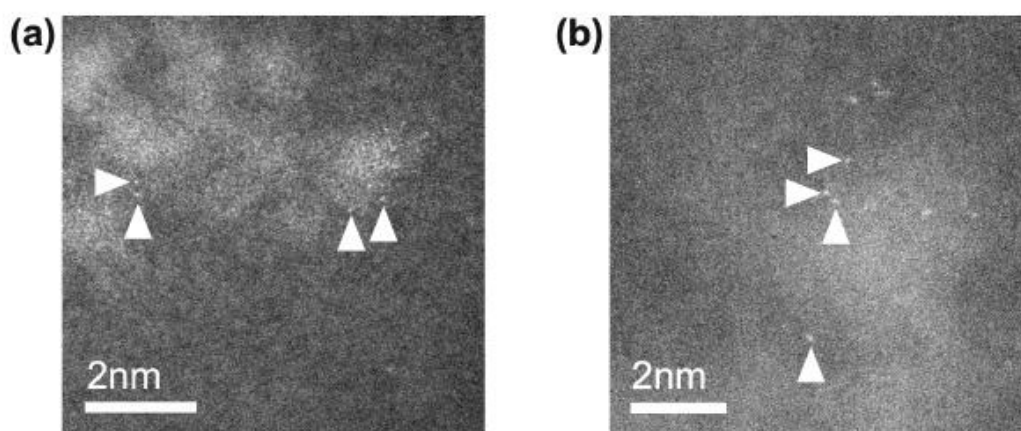

Figure 5. ADF images of atomic clusters located using high-magnification STEM. Single atoms are identified by arrowheads.

As the fraction of the incident electron beam scattered by an atom is characteristic of its atomic number, by carefully measuring this value it is possible to identify its elemental species from images of the type shown in Figure 5. The success of the quantification procedure used in this paper relies upon accurate measurements of the ADF detector parameters. The experimental image and detector map were both analyzed using the AbsoluteIntegrator v1.6.4 code (developed as part of the ESTEEM2 project). The results are shown in Figure 6, indicating that for a single platinum atom only a few percent of the incident beam electrons are scattered to the HAADF detector.
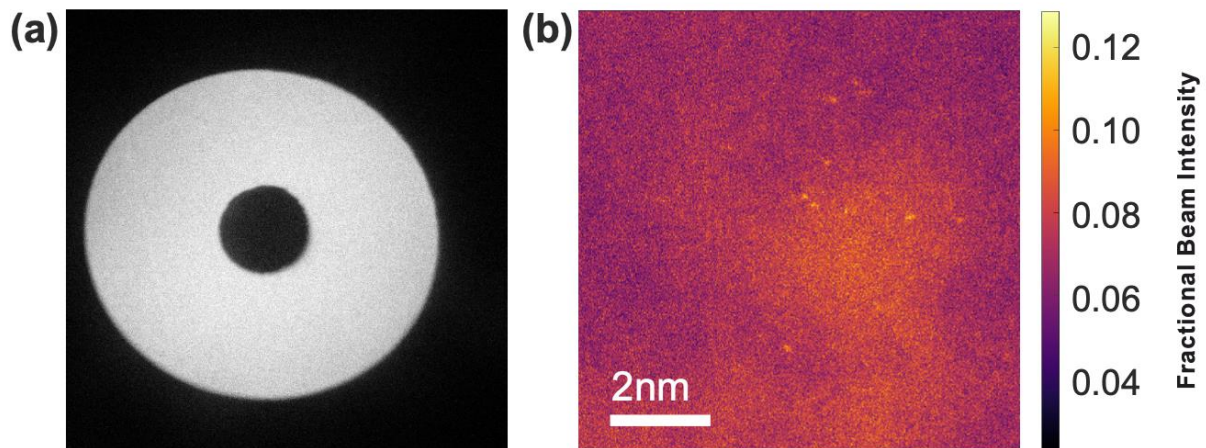

Figure 6. *(a)* Response map of the upper ADF detector in the Oxford JEOL ARM-200F. (b) Atomic cluster image converted to units of fractional beam intensity. The most intense areas indicate as much as 12% of the beam is scattered to the HAADF detector at some probe positions.

Placing single-atom images on this absolute scale allows for direct comparison between experimental measurements of elastic scattering strength and those predicted by simulation. In particular, it is often desirable to measure a partial scattering cross-section σ_{ADF} for all or part of the image; this parameter has been shown to be robust to microscope aberrations, and suitable for identifying atomic species. Analysis of the cross-sections for the observed single atoms confirms that they are Pt (Figure 7). The predicted partial scattering cross section values for lighter and more biologically abundant elements are more than an order of magnitude smaller than measured from experimental images. The amount of high-angle scattering generated by these single atoms is therefore consistent with a high-Z element such as platinum, presumed to be present in the cell due to oxaliplatin administration.
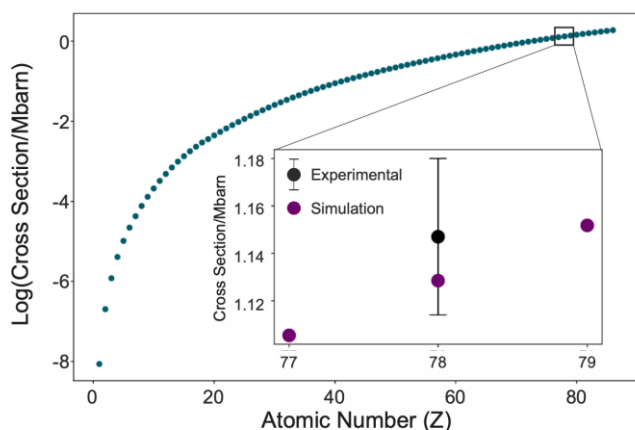
7

Figure 7. Logarithmic plot of simulated ADF scattering cross-section against atomic number. The inset graph shows expected cross-sections for iridium, platinum and gold (Z=77, 78 and 79 respectively). Experimental data with an error bar of one standard deviation are also shown in black.

Electron tomography of nanoparticles (ANT)

Anisotropic Au nanoparticles are of great interest in the field of medicine, since their plasmonic properties can be exploited during e.g. photothermal ablation of cancer cells. These properties are strongly dependent on the morphology and 3D structure of such nanoparticles. Although nanoparticle synthesis can be performed with high control, it is of equal importance to investigate, if the predefined shapes are maintained, when the nanoparticles are exposed to realistic environmental conditions. For example, a relevant question is what happens to the anisotropic morphology, when a nanoparticle absorbs heat because of laser illumination?

Investigation of a 3D structure can be performed using electron tomography, a technique, where the 3D structure of a (nano)material is recovered based on a series of 2D projection images, covering a tilt range that is as large as possible. Electron tomography has been proven to be of great use to investigate a very broad range of materials and even atomic resolution in 3D can be obtained nowadays. However, an inherent limitation of the technique is that the acquisition is very time consuming. Approximately 1 hour or more is required to collect the necessary data for 3D reconstruction. This is too long to capture the transformation that occurs, when nanoparticles are exposed to higher temperatures. We therefore recently developed fast HAADF-STEM tomography, an approach, where continuous tilting of the holder enables us to reduce the acquisition time for a tilt series to a few minutes [1,2]. By combination of the approach with a micro-electromechanical system (MEMS) Denssolutions heating holder, able to tilt over a range of ±80°, the technique has been proven to be of great interest to measure transformations of morphology and composition as a function of temperature. An example is provided in Figure 8, where the transformation of a Au nanostar after specific heating steps is presented. By quantification of the HAADF-STEM contrast, also changes in composition at high temperature could be investigated, as illustrated in Figure 9 [3]. Such changes will again affect the plasmonic properties and eventually the use of these particles for medical application. Although 3D investigations at high temperature are of great interest, it is important to realize that the interpretation of in situ experiments is not straightforward since the electron beam can impact the outcome of such measurements. For example, ligands surrounding metal nanoparticles transform into a protective carbon layer upon electron beam irradiation and may impact the apparent thermal stability

during in situ heating experiments. Therefore, caution is needed when performing 3D in situ heating experiments and comparison of experiments are necessary [4].
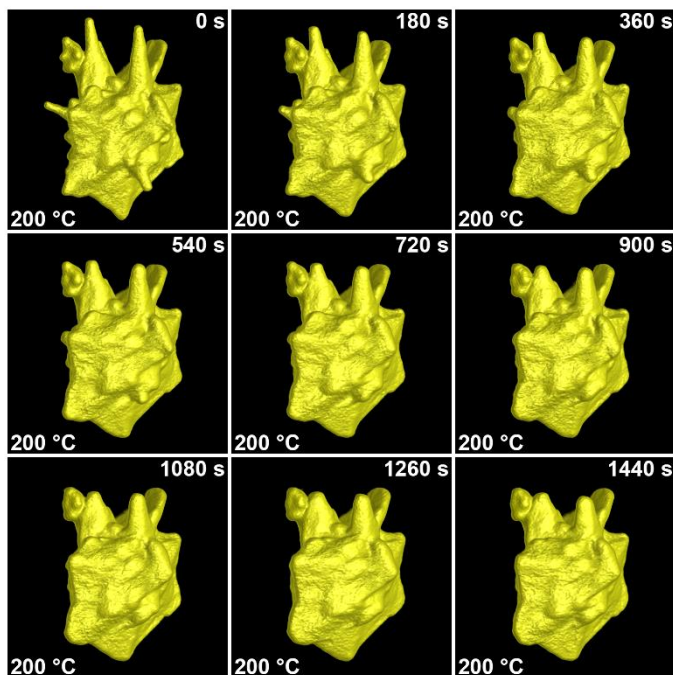

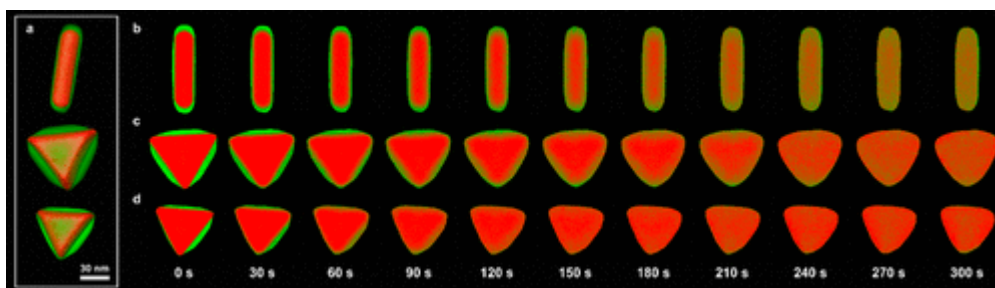Figure 8: 3D visualizations of a Au nanostar after specific intervals of heating at 200°C.

Figure 9: (a) Visualizations of 3D reconstructions for the particles studied in this work. (b– d) Slices through the 3D reconstructions of elemental distributions inside the nanorod, the symmetric, and the asymmetric nanotriangles, respectively, at different stages of alloying at 450 °C

References:

1. "Three-Dimensional Nanoparticle Transformations Captured by an Electron Microscope". Albrecht W, Van Aert S, Bals S, Accounts Of Chemical Research 54, 1189 (2021). http://doi.org/10.1021/acs.accounts.0c00711

2. "Fast Electron Tomography for Nanomaterials". Albrecht W, Bals S, Journal Of Physical Chemistry C , acs.jpcc.0c08939 (2020).   http://doi.org/10.1021/acs.jpcc.0c08939

3. "Quantitative 3D Characterization of Elemental Diffusion Dynamics in Individual Ag@Au Nanoparticles with Different Shapes". Skorikov A, Albrecht W, Bladt E, Xie X, van der Hoeven JES, van Blaaderen A, Van Aert S, Bals S, Acs Nano 13, 13421 (2019). http://doi.org/10.1021/acsnano.9b06848

4. "Effectiveness of reducing the influence of CTAB at the surface of metal nanoparticles during in situ heating studies by TEM". De Meyer R, Albrecht W, Bals S, Micron 144, 103036 (2021).   http://doi.org/10.1016/j.micron.2021.103036